

We are IntechOpen, the world's leading publisher of Open Access books Built by scientists, for scientists

6,900

Open access books available

186,000

International authors and editors

200M

Downloads

Our authors are among the

154

Countries delivered to

TOP 1%

most cited scientists

12.2%

Contributors from top 500 universities



WEB OF SCIENCE™

Selection of our books indexed in the Book Citation Index
in Web of Science™ Core Collection (BKCI)

Interested in publishing with us?
Contact book.department@intechopen.com

Numbers displayed above are based on latest data collected.
For more information visit www.intechopen.com



Ultrafast Electron and Hole Dynamics in CdSe Quantum Dot Sensitized Solar Cells

Qing Shen¹ and Taro Toyoda²

¹PRESTO, Japan Science and Technology Agency (JST)

²The University of Electro-Communications
Japan

1. Introduction

A potential candidate for next-generation solar cells is dye-sensitized solar cells (DSSCs). Much attention has been directed toward DSSCs employing nanostructured TiO₂ electrodes and organic-ruthenium dye molecules as the light-harvesting media. The high porosity of nanostructured TiO₂ film enables a large concentration of the sensitizing dye molecules to be adsorbed. The attached dye molecules absorb light and inject electrons into the TiO₂ conduction band upon excitation. The electrons are then collected at a back conducting electrode, generating a photocurrent. DSSCs exhibit high photovoltaic conversion efficiencies of about 11% and good long-term stability. In addition, they are relatively simple to assemble and are low-cost (O'Regan & Grätzel, 1991; Grätzel, 2003; Chiba et al., 2006). However, in order to replace conventional Si-based solar cells in practical applications, further effort is needed to improve the efficiency of DSSCs. A great amount of work has been done on controlling the morphology of the TiO₂ electrodes by employing ordered arrays of nanotubes, nanowires, nanorods and inverse opal structures (Adachi et al., 2003; Paulose et al., 2006; Law et al., 2005; Song et al., 2005; Nishimura et al., 2003) in order to improve the electron transport and collection throughout the device. Another important factor in improving the performance of DSSCs is the design of the photosensitizer. The ideal dye photosensitizer for DSSCs should be highly absorbing across the entire solar light spectrum, bind strongly to the TiO₂ surface and inject photoexcited electrons into the TiO₂ conduction band efficiently. Many different dye compounds have been designed and synthesized to fulfill the above requirements. It is likely that the ideal photosensitizer for DSSCs will only be realized by co-adsorption of a few different dyes, for absorption of visible light, near infrared (NIR) light, and/or infrared (IR) light (Polo et al., 2004; Park et al., 2011). However, attempts to sensitize electrodes with multiple dyes have achieved only limited success to date.

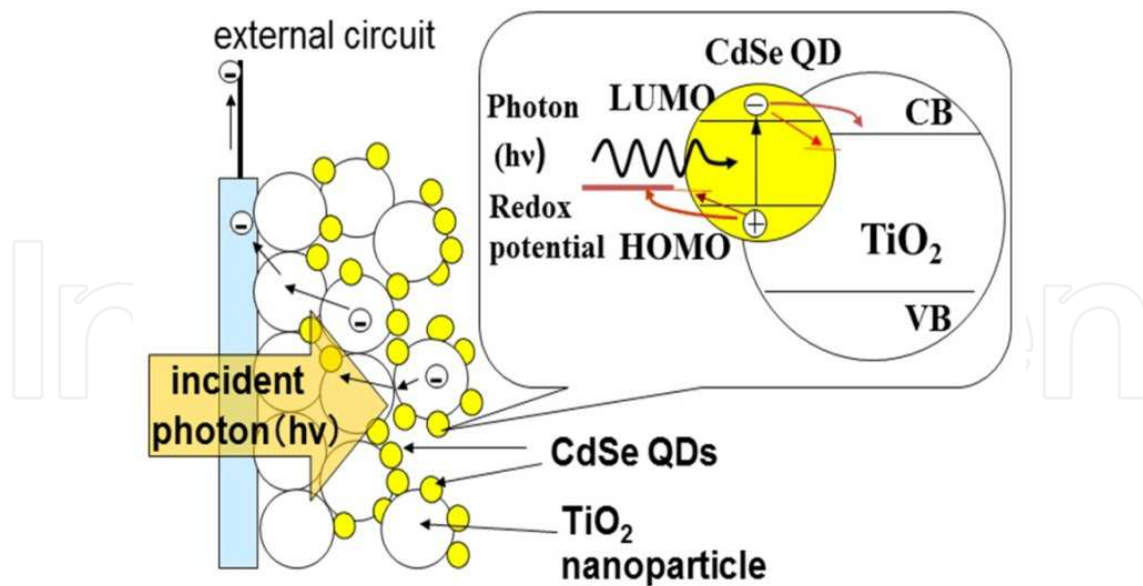
Narrow-band-gap semiconductor quantum dots (QDs), such as CdS, CdSe, PbS, and InAs, have also been the subject of considerable interest as promising candidates for replacing the sensitizer dyes in DSSCs (Vogel et al., 1990, 1994; Toyoda et al., 1999, 2003; Peter et al., 2002; Plass et al., 2002; Shen et al., 2004a, 2004b, 2006a, 2006b, 2008a, 2008b, 2010a, 2010b; Yu et al., 2006; Robel et al., 2006; Niitsoo et al., 2006; Diguna, et al., 2007a, 2007b; Kamat, 2008, 2010; Gimenez et al., 2009; Mora-Sero et al., 2009, 2010). These devices are called QD-sensitized solar cells (QDSCs) (Nozik, 2002, 2008; Kamat, 2008). The use of semiconductor QDs as sensitizers

has some unique advantages over the use of dye molecules in solar cell applications (Nozik, 2002, 2008). First, the energy gaps of the QDs can be tuned by controlling their size, and therefore the absorption spectra of the QDs can be tuned to match the spectral distribution of sunlight. Secondly, semiconductor QDs have large extinction coefficients due to the quantum confinement effect. Thirdly, these QDs have large intrinsic dipole moments, which may lead to rapid charge separation. Finally, semiconductor QDs have potential to generate multiple electron-hole pairs with one single photon absorption (Nozik, 2002; Schaller, 2004), which can improve the maximum theoretical thermodynamic efficiency for photovoltaic devices with a single sensitizer up to ~44% (Hanna et al., 2006). However, at present, the conversion efficiency of QDSCs is still less than 5% (Mora-Sero, et al., 2010; Zhang, et al., 2011). So, fundamental studies on the mechanism and preparation of QDSCs are still necessary and very important.

In a semiconductor quantum dot-sensitized solar cell (QDSC), as the first step of photosensitization, a photoexcited electron in the QD should rapidly transfer to the conduction band of TiO₂ electrode and a photoexcited hole should transfer to the electrolyte (Scheme 1). Thus charge separation of the photoexcited electrons and holes in the semiconductor QDs and the electron injection process are key factors for the improvement of the photocurrents in the QDSCs. In this sense, the study on the photoexcited carrier dynamics in the QDs is very important for improving the conversion efficiency of the solar cell. To date, the information on the carrier dynamics of semiconductor QDs adsorbed on TiO₂ electrode is limited, although a few studies have been carried out for CdS, CdSe and InP QDs using a transient absorption (TA) technique (Robel et al., 2006, 2007; Tvrđy et al., 2011; Blackburn et al., 2003, 2005). Most of them focused on the electron transfer process and the measurements mostly were carried out in either dispersed colloidal systems or dry electrodes. In recent years, the authors' group has been applying an improved transient grating technique (Katayama et al., 2003) to study the photoexcited carrier dynamics of semiconductor nanomaterials, such as TiO₂ nanoparticles with different crystal structures and CdSe QDs adsorbed onto TiO₂ and SnO₂ nanostructured electrodes (Shen et al., 2005, 2006, 2007, 2008, 2010). The improved TG technique is a simple and highly sensitive time-resolved optical technique and has proved to be powerful for measuring various kinds of dynamics, such as population dynamics and excited carrier diffusion. Comparing to the TA technique, the improved TG technique has a higher sensitivity and measurements under lower light intensity are possible (Katayama et al., 2003; Shen et al., 2007, 2010a). This fact is very important for studying the carrier dynamics of QDs used in QDSCs under the conditions of lower light intensity similar to sun light illumination. The improved TG technique is also applicable to samples with rough surfaces, like the samples used in this study.

This chapter will focus on the ultrafast photoexcited electron and hole dynamics in CdSe QD adsorbed TiO₂ electrodes employed in QDSCs characterized by using the improved TG technique. CdSe QDs were adsorbed on TiO₂ nanostructured electrodes with different adsorption methods. The following issues will be discussed:

1. Pump light intensity dependence of the ultrafast electron and hole dynamics in the CdSe QDs adsorbed onto TiO₂ nanostructured electrodes;
2. Separation of the ultrafast electron and hole dynamics in the CdSe QDs adsorbed onto TiO₂ nanostructured electrodes;
3. Electron injection from CdSe QDs to TiO₂ nanostructured electrode;
4. Changes of carrier dynamics in CdSe QDs adsorbed onto TiO₂ electrodes versus adsorption conditions;
5. Effect of surface modification on the ultrafast carrier dynamics and photovoltaic properties of CdSe QD sensitized TiO₂ electrodes.



Scheme 1. Electron-hole pairs are generated in semiconductor QDs after light absorption. Then photoexcited electrons in the semiconductor QDs are injected to the conduction band of TiO_2 and/or trapped by surface or interface states. The photoexcited holes are scavenged by reducing species in the electrolyte and/or trapped by surface or interface states. The nanostructured TiO_2 is employed as an electron conductor and electrons transport in TiO_2 to a transparent conductive oxide (TCO) substrate, while the electrolyte is used as a hole transporter and holes are transported to a counter electrode.

2. Electron and hole dynamics in CdSe QDs adsorbed onto TiO_2 electrodes

2.1 Preparation methods of CdSe QD adsorbed TiO_2 nanostructured electrodes

The method for preparing the TiO_2 electrodes has been reported in a previous paper (Shen et al., 2003). A TiO_2 paste was prepared by mixing 15 nm TiO_2 nanocrystalline particles (Super Titania, Showa Denko; anatase structure) and polyethylene glycol (PEG) (molecular weight (MW): 500,000) in pure water. The resultant paste was then deposited onto transparent conducting substrates (F-doped SnO_2 (FTO), sheet resistance = 10 Ω/sq). The TiO_2 films were then sintered in air at 450 $^\circ\text{C}$ for 30 min to obtain good necking. The highly porous nanostructure of the TiO_2 films (the pore sizes are of the order of a few tens of nanometers) was confirmed through scanning electron microscopy (SEM) images.

CdSe QDs can be adsorbed onto the TiO_2 nanostructured electrodes by using the following methods:

1. Chemical bath deposition (CBD) method (Hodes et al., 1994; Shen et al., 2008)
Firstly, for the Se source, an 80 mM sodium selenosulphate (Na_2SeSO_3) solution was prepared by dissolving elemental Se powder in a 200 mM Na_2SO_3 solution. Secondly, 80 mM CdSO_4 and 120 mM of the trisodium salt of nitrilotriacetic acid ($\text{N}(\text{CH}_2\text{COONa})_3$) were mixed with the 80 mM Na_2SeSO_3 solution in a volume ratio of 1:1:1. The TiO_2 films were placed in a glass container filled with the final solution at 10 $^\circ\text{C}$ in the dark for various times to promote CdSe adsorption.
2. Successive ionic layer adsorption-reaction (SILAR) method (Guijarro et al., 2010a)
In situ growth of CdSe QDs using the SILAR method was carried out by successive immersion of TiO_2 electrodes in ionic precursor solutions of cadmium and selenium.

Aqueous solutions were employed in all cases. A 0.5 M $(\text{CH}_3\text{COO})_2\text{Cd}$ (98.0%, Sigma-Aldrich) solution was used as the cadmium source, while a sodium selenosulfate (Na_2SeSO_3) solution was used as the selenium precursor. The sodium selenosulfate solution was prepared by heating under reflux for 1h a mixture of 1.6 g of Se powder, 40 mL of 1 M Na_2SO_3 (98.0%, Alfa Aesar) and 10 mL of 1 M NaOH. The resulting solution was filtered and mixed with 40 mL of 1M CH_3COONa (99.0+%, Fluka) solution, and finally was stored in the dark. The pH of the sodium selenosulfate solution was optimized to improve the QD deposition rate by using 0.25 M H_2SO_4 and/or 0.1 M NaOH stock solutions.

3. Direct adsorption (DA) of previously synthesized QDs (Guijarro et al., 2010b)
Colloidal dispersions of CdSe QDs capped with trioctylphosphine (TOP) were prepared by a solvothermal route which permits size control. DA of CdSe QDs was achieved by immersion of TiO_2 electrodes in a CH_2Cl_2 (99.6%, Sigma Aldrich) CdSe QD dispersion, using soaking times ranging from 1 h to 1 week.
4. Linker assisted adsorption (LA) of previously synthesized QDs (Guijarro et al., 2010b)
LA was performed employing p-mercaptobenzoic acid (MBA; 90%, Aldrich), cysteine (97%, Aldrich), and mercaptopropionic acid (MPA; 99%, Aldrich) as molecular wires. First, the linker was anchored to the TiO_2 surface by immersion in saturated toluene solutions of cysteine (5 mM) or MBA (10 mM) for 24 h. Secondly, these electrodes were washed with pure toluene for $\frac{1}{2}$ h to remove the excess of the linker. Finally, the modified electrodes were transferred to a toluene CdSe QD dispersion for 3 days, to ensure QD saturation. The procedure for modification of TiO_2 with MPA has previously been reported (Guijarro et al., 2009).

After the CdSe QD adsorption, the samples were coated with ZnS by alternately dipping them three times in 0.1 M $\text{Zn}(\text{CH}_2\text{COO})$ and 0.1 M Na_2S aqueous solutions for 1 minute for each dip (Yang et al., 2003; Diguna, et al., 2007a; Shen et al., 2008).

2.2 An improved transient grating (TG) technique

The transient grating (TG) method is a well-established laser spectroscopic technique of four wave mixing (Eichler et al., 1986; Harata et al., 1999). In the TG method, two time-coincident short laser pulses (pump beams) with the same wavelength and intensity intersect with an angle in a sample to generate an optical interference pattern at the intersection. Interaction between the light field and the material results in a spatially periodic modulation of the complex refractive index, which works like a transient diffraction grating for a third laser pulse (probe beam) incident to the photoexcited region. Then, by measuring the time dependence of the diffraction light of the probe beam, dynamics of the transient grating produced in the sample can be monitored. The TG technique is a powerful tool for detecting population dynamics (Rajesh et al., 2002), thermal diffusion (Glorieux et al., 2002), diffusion of photoexcited species (Terazima et al., 2000), energy transfer from photoexcited species to liquids (Miyata et al, 2002), structural or orientational relaxation (Glorieux et al., 2002), the sound velocity of liquids (Ohmor et al., 2001), and so on. Although this technique provides valuable information, it presents some technical difficulties for general researchers (Harata et al., 1999). First, the three beams must overlap on a small spot, typically within a spot diameter of less than 100 μm on a sample, and each beam must be temporally controlled. This is very difficult for pulsed laser beams, especially for those with a pulse width of ~ 100 femtoseconds. Secondly, since the diffraction of the probe beam, namely the signal, is quite weak, it is difficult to find the diffraction beam during the measurements. Thirdly, for a solid sample, the surface must be optically smooth. It is almost impossible to measure a sample with a rough surface by using the conventional TG technique.

In 2003, Katayama and co-workers (Katayama et al., 2003; Yamaguchi et al., 2003) proposed an improved TG technique (it was also called a lens-free heterodyne TG (LF-HD-TG) or a near field heterodyne TG (NF-HD-TG) technique in some papers), which overcomes the difficulties that exist in the conventional TG technique. The improved TG technique features (1) simple and compact optical equipment and easy optical alignment and (2) high stability of phase due to the short optical path length of the probe and reference beams. This method is thought to be versatile with applicability to many kinds of sample states, namely opaque solids, scattering solids with rough surfaces, transparent solids, and liquids, because it is applicable to transmission and reflection-type measurements. The principle of the improved TG technique has been explained in detail in the previous papers (Katayama et al., 2003; Yamaguchi et al., 2003) and is only described briefly here. Unlike the conventional TG technique, only one pump beam and one probe beam without focusing are needed in the improved TG technique. The pump beam is incident on the transmission grating. Then, the spatial intensity profile of the pump beam is known to have an interference pattern in the vicinity of the other side of the transmission grating, and the interference pattern has a grating spacing that is similar to that of the transmission grating. When a sample is brought near the transmission-grating surface, it can be excited by the optical interference pattern. The refractive index of the sample changes according to the intensity profile of the pump light and the induced refractive index profile functions as a different type of transiently generated grating. When the probe beam is incident in a manner similar to that of the pump beam, it is diffracted both by the transmission grating (called a reference light) and the transiently generated grating (called a signal light). In principle, the two diffractions progress along the same direction; therefore, these two diffractions interfere, which is detected by a detector positioned at a visible diffraction spot of the reference beam.

In the improved TG technique used for studying the ultrafast carrier dynamics of semiconductor QDs, the laser source was a titanium/sapphire laser (CPA-2010, Clark-MXR Inc.) with a wavelength of 775 nm, a repetition rate of 1 kHz, and a pulse width of 150 fs. The light was separated into two parts. One of them was used as a probe pulse. The other was used to pump an optical parametric amplifier (OPA) (a TOAPS from Quantronix) to generate light pulses with a wavelength tunable from 290 nm to 3 μm used as pump light in the TG measurement. The probe pulse wavelength was 775 nm.

2.3 Power dependence of carrier dynamics in CdSe QDs adsorbed onto TiO₂ electrodes

As described in depth in previous papers (Katayama et al., 2003; Shen et al., 2005, 2007), the TG signal is directly proportional to the change in the refractive index occurring in the sample ($\Delta n(t)$) upon photoexcitation. In the timescale of these experiments less than 1 ns, assuming Drude's model, the refractive index change, i.e., the TG signal intensity for CdSe QD adsorbed samples, will be a linear function of the concentration of photogenerated carriers (electrons and holes in CdSe QDs, i.e., $N_{e,\text{CdSe}}$ and $N_{h,\text{CdSe}}$, and injected electrons in TiO₂, i. e., N_{e,TiO_2}), as follows (Guijarro et al., 2010a, 2020b):

$$\Delta n(t) = \frac{1}{2n_{0,\text{CdSe}}} \left(\frac{-N_{e,\text{CdSe}}(t)e^2}{m_{e,\text{CdSe}}\omega_p^2\varepsilon_0} \right) + \frac{1}{2n_{0,\text{CdSe}}} \left(\frac{-N_{h,\text{CdSe}}(t)e^2}{m_{h,\text{CdSe}}\omega_p^2\varepsilon_0} \right) + \frac{1}{2n_{0,\text{TiO}_2}} \left(\frac{-N_{e,\text{TiO}_2}(t)e^2}{m_{e,\text{TiO}_2}\omega_p^2\varepsilon_0} \right) \quad (1)$$

where ω_p is the radial probe frequency, e is the elementary charge, ε_0 is free-space permittivity, and $n_{0,\text{CdSe}}$ (2.7) and n_{0,TiO_2} (2.5) are the refractive indices of CdSe and TiO₂, respectively. The important feature of the TG signal is that both the photoexcited electron

and hole carrier densities contribute to the signal. In principle, the exact contribution on $\Delta n(t)$ by each carrier depends inversely on its carrier effective mass. According to the Drude theory (Kashiski et al., 1989; Kim et al., 2009), it can be considered that only free photoexcited electrons and holes are responsible for the population grating signals. For CdSe, the effective masses of electrons and holes are $0.13m_0$ and $0.44m_0$ (m_0 is the electron rest mass), respectively (Bawendi et al., 1989), so both the photoexcited electron and hole carrier densities in the CdSe QDs contribute to the signal. It is known that the effective mass of electrons for TiO₂ is about $30 m_0$, which is about two orders larger than that for CdSe. Therefore, the TG signal due to the injected electrons in TiO₂ (no holes injected into TiO₂) can be ignored (Shen et al., 2005, 2006a, 2007, 2008a, 2010a).

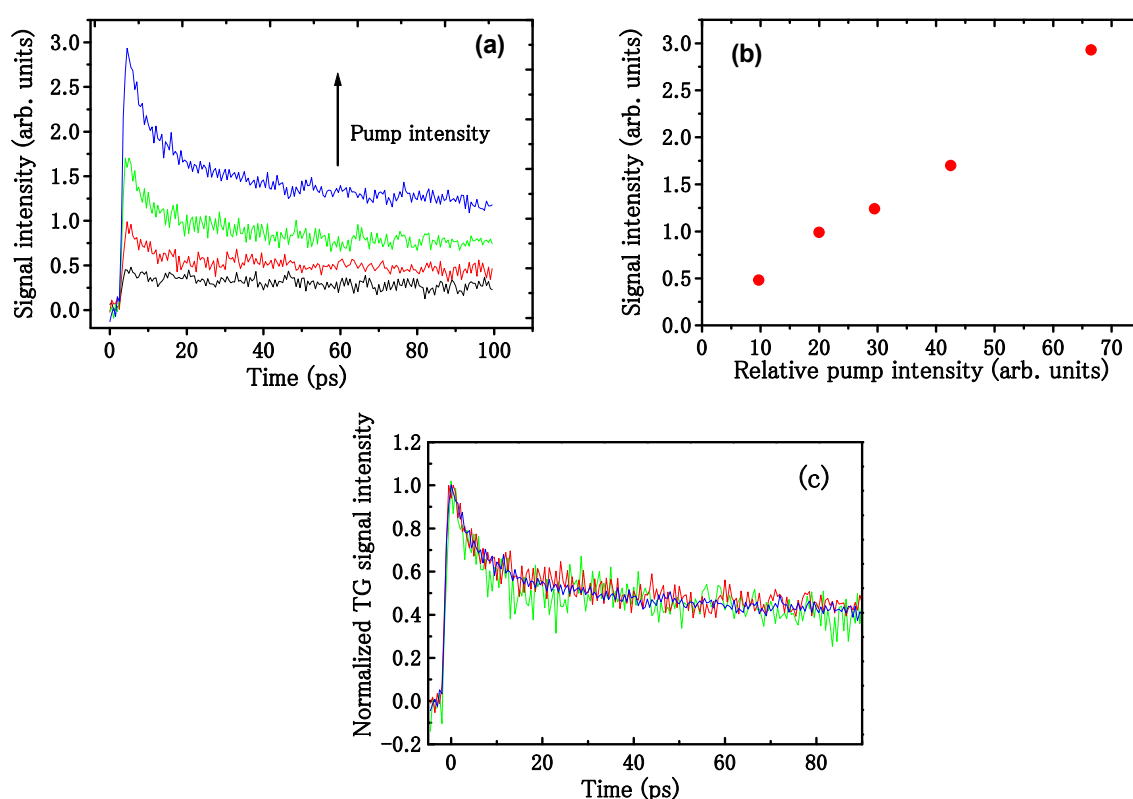


Fig. 1. Dependence of the TG kinetics of CdSe QDs adsorbed onto nanostructured TiO₂ films (CBD method and the CdSe adsorption time was 24 h) on the pump light intensity (a); Dependence of the TG peak intensity on the pump light intensity (b); Normalized TG kinetics measured with different pump light intensities (c) (Shen et al., 2010a).

For a semiconductor material, usually, there are three kinds of photoexcited carrier relaxation dynamics. The first one is a one-body recombination, which is trapping and/or transfer of photoexcited electrons and holes. In this case, the lifetimes of the photoexcited electrons and holes are independent of the pump light intensity. The second one is a two-body recombination, which is a radiative recombination via electron and hole pairs. The third one is a three-body recombination, which is an Auger recombination via two electrons and one hole, or via one electron and two holes. In the latter two cases, the lifetimes of photoexcited electrons and holes are dependent on the pump light intensity. In order to determine what kinds of photoexcited carrier dynamics are reflected in the TG kinetics, we first confirmed many-body recombination processes such as the Auger recombination

process existed or not under our experimental conditions. For this purpose, we measured the dependence of the TG kinetics on the pump intensity (from 2.5 to 16.5 $\mu\text{J}/\text{pulse}$) for CdSe QD adsorbed TiO_2 electrodes (Figure 1) (Shen et al., 2010a). As shown in Fig. 1, we found that the dependence of the maximum signal intensity on the pump intensity was linear, and that the waveforms of the responses overlapped each other very well when they were normalized at the peak intensity. These results mean that the decay processes measured in the TG kinetics were independent of the pump intensity under our experimental conditions, and many-body recombination processes could be neglected. Therefore, it is reasonable to assume that the decay processes of photoexcited electrons and holes in the CdSe QDs are due to one-body recombination processes such as trapping and transfer under our experimental conditions.

2.4 Separation of the ultrafast electron and hole dynamics in the CdSe QDs adsorbed onto TiO_2 nanostructured electrodes

Figure 2 shows a typical kinetic trace of the TG signal of CdSe QDs adsorbed onto a TiO_2 nanostructured film (prepared by CBD method for 24 h adsorption) measured in air. The vertical axis was plotted on a logarithmic scale. Three decay processes (indicated as A, B, and C in Fig. 2) can be clearly observed. We found that the TG kinetics shown in Fig. 2 could be fitted very well with a double exponential decay plus an offset, as shown in eq. (2):

$$y = A_1 e^{-t/\tau_1} + A_2 e^{-t/\tau_2} + y_0 \quad (2)$$

where A_1 , A_2 and y_0 are constants, and τ_1 and τ_2 are the time constants of the two decay processes (A and B in Fig. 2). Here, the constant term y_0 corresponds to the slowest decay process (C in Fig. 2), in which the decay time (in the order of ns) is much larger than the time scale of 100 ps measured in this study. The time constants of the fast (τ_1) and slow (τ_2) decay processes of photoexcited carriers in air are 6.3 ps and 82 ps, respectively (Table 1). As mentioned above, τ_1 and τ_2 are independent of the pump intensity under our experimental conditions, so the three decay processes are mostly due to one-body recombination such as carrier trapping and carrier transfer.

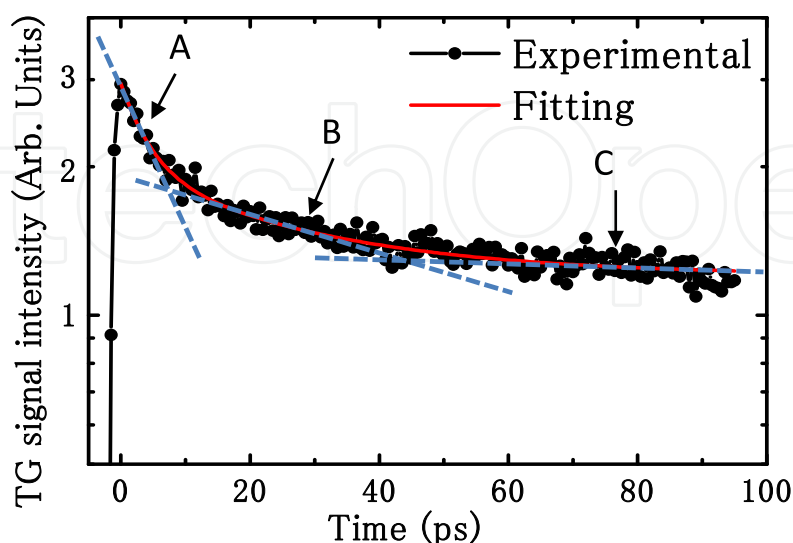


Fig. 2. TG kinetics of CdSe QDs adsorbed onto a nanostructured TiO_2 film measured in air. The vertical axis is plotted on a logarithmic scale. Three decay processes A, B and C can be clearly observed (Shen et al., 2010a).

In order to separate the photoexcited electron dynamics and hole dynamics that make up the TG kinetics, the TG kinetics of the same sample was measured both in air and in a Na_2S aqueous solution (hole acceptor) (1 M) (Shen et al., 2010a). As shown in Fig. 3, a large difference can be clearly observed between the TG responses measured in air and in the Na_2S solution. By normalizing the two TG responses at the signal intensity of 90 ps, we found that they overlapped with each other very well for time periods of longer than 15 ps, but the fast decay process apparently disappeared when the time period was less than 10 ps in the TG kinetics measured in the Na_2S solution (hole acceptor). This great difference can be explained as follows. In air, both hole and electron dynamics in the CdSe QDs could be measured in the TG kinetics. In the Na_2S solution, however, photoexcited holes in the CdSe QDs will transfer quickly to the electrolyte and only electron dynamics should be measured in the TG kinetics. Therefore, the “apparent disappearance” of the fast decay process in the Na_2S solution implies that the hole transfer to S^{2-} ions, which are supposed to be strongly adsorbed onto the CdSe QD surface, can be too fast in these circumstances as indicated by Hodes (Hodes, 2008) and therefore could not be observed under the temporal resolution (about 300 fs) of our TG technique. This observation is particularly important, because the result directly demonstrated that the transfer of holes to sulfur hole acceptors that are strongly adsorbed on the QD surface could approach a few hundreds of fs. An earlier study on the dynamics of photogenerated electron-hole pair separation in surface-space-charge fields at GaAs(100) crystal/oxide interfaces using a reflective electro-optic sampling method

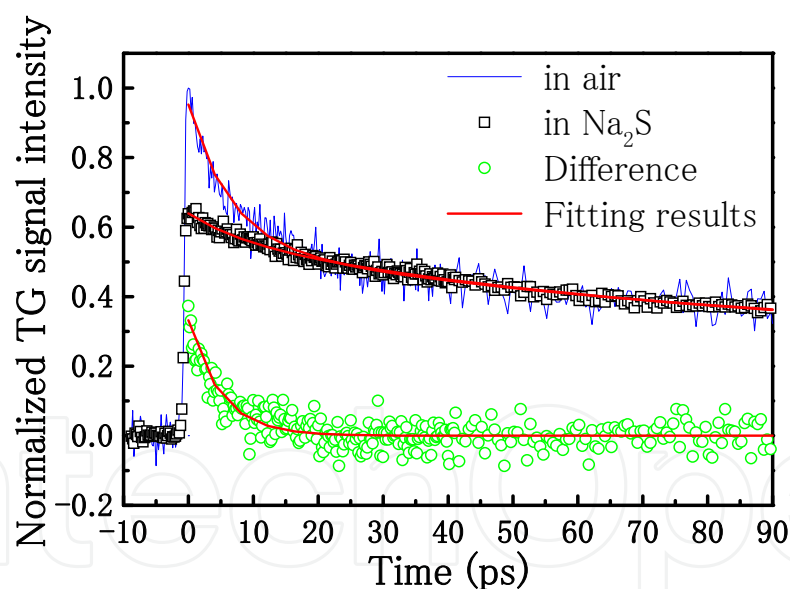


Fig. 3. TG responses of the CdSe QDs adsorbed onto nanostructured TiO_2 films measured in air (-) and in Na_2S solution (\square) as well as their “difference response” (\circ) (Shen et al., 2010a).

showed that the hole carrier transit time was faster than 500 fs (Min et al., 1990). We believe an ultrafast hole transfer time from the QDs to hole acceptors that are strongly adsorbed on the QD surface is a more feasible and reasonable explanation, since photoexcited holes can more easily reach the surface of QDs with diameters of a few nm. The TG response measured in the Na_2S solution, which is considered to only relate to electron dynamics as mentioned above, can be fitted well with eq. (2). As shown in Table 1, besides the slower decay process, a faster decay process with a decay time of 9 ps was also detected in the TG

response measured in the Na₂S solution. Such a faster decay process with a characteristic time of a few picoseconds in the TG response measured in the Na₂S solution was considered to correspond to electron transfer from the QDs in direct contact with the TiO₂ (first layer of deposited QDs) (Guijarro et al., 2010a, 2010b). It is worth noting that the relative intensity A_1 (0.07) measured in the Na₂S solution is much smaller compared to the A_1 (0.39) measured in air and it could be ignored here. The slower relaxation process in the TG response was not influenced by the presence of the Na₂S solution, as shown in Fig. 3. The decay time τ_2 (85 ps) and the relative intensity A_2 (0.31) for the slower decay process in the TG response measured in the Na₂S solution are almost the same as those measured in air (Table 1). The slower electron relaxation mostly corresponds to electron transfer from the CdSe QDs to TiO₂ and trapping at the QD surface states, in which the decay time depends to a great extent on the size of the QDs and the adsorption method that is used (Guijarro et al., 2010a, 2010b; Shen et al., 2006, 2007; Diguna et al., 2007b). The slowest decay process (with a time scale of ns) may mostly result from the non-radiative recombination of photoexcited electrons with defects that exist at the CdSe QD surfaces and at the CdSe/CdSe interfaces.

The difference between the two TG responses measured in air and in Na₂S solution (normalized for the longer time), which was termed the “difference response”, is believed to correspond to the photoexcited hole dynamics in the CdSe QDs measured in air. As shown in Fig. 3, the difference response decays very fast and disappears around 10 ps and can be fitted very well with a one-exponential decay function with a decay time of 5 ps (Table 1). Thus, we did well in separating the dynamics of photoexcited electrons and holes in the CdSe QDs and found that the hole dynamics were much faster than those of electrons. Some papers have also reported that the hole relaxation time is much faster than the electron relaxation time in CdS and CdSe QDs (Underwood et al., 2001; Braun et al., 2002). In air, the fast hole decay process with a time scale of about 5 ps can be considered as the trapping of holes by the CdSe QD surface states. This result is in good agreement with the experimental results obtained by a femtosecond fluorescence “up-conversion” technique (Underwood et al., 2001).

Thus, by comparing the TG responses measured in air and in a Na₂S solution (hole acceptor), we succeeded in separating the dynamic characteristics of photoexcited electrons and holes in the CdSe QDs. We found that charge separation in the CdSe QDs occurred over a very fast time scale from a few hundreds of fs in the Na₂S solution via hole transfer to S²⁻ ions to a few ps in air via hole trapping.

| TG kinetics | A_1 | τ_1 (ps) | A_2 | τ_2 (ps) | y_0 |
|----------------------|------------|---------------|------------|---------------|------------|
| In air | 0.39± 0.01 | 6.3±0.4 | 0.29 ±0.01 | 82 ±7 | 0.27± 0.01 |
| In Na ₂ S | 0.07± 0.01 | 9 ±1 | 0.31± 0.01 | 85 ±1 | 0.25± 0.01 |
| Difference | 0.33± 0.01 | 5.0± 0.3 | - | - | - |

Table 1. Fitting results of the TG responses of CdSe QDs adsorbed onto nanostructured TiO₂ films measured in air and in Na₂S solution (hole acceptor) as well as their “difference response” as shown in Fig. 3 with a double exponential decay equation (eq. (2)). τ_1 and τ_2 are time constants; A_1 , A_2 and y_0 are constants (Shen et al., 2010a).

2.5 Electron injection from CdSe QDs to TiO₂ nanostructured electrode

To investigate the electron transfer rate from CdSe QDs to TiO₂ electrodes, Shen and co-workers measured the TG kinetics of CdSe QDs adsorbed on both nanostructured TiO₂ electrodes and glass substrates under the same deposition conditions (Shen et al., 2008).

Figure 4 shows the TG kinetics (pump beam wavelength: 388 nm) of CdSe QDs adsorbed on a TiO₂ nanostructured electrode and on a glass substrate (CBD method). The average diameter of the CdSe QDs was about 5.5 nm for both kinds of substrates. The TG kinetics were fitted to a double exponential decay function (Eq. (3)) using a least-squares fitting method, convoluting with a 1ps Gaussian representing the laser pulse.

$$y = A_1 e^{-t/\tau_1} + A_2 e^{-t/\tau_2} \quad (3)$$

where A_1 and A_2 are constants, and τ_1 and τ_2 are the time constants of the two decay processes, respectively.

The fast decay time constants τ_1 were obtained to be 2.3 ps for both the two kinds of substrates. The slow decay time constants τ_2 were obtained to be approximately 140 ps and 570 ps for the CdSe QDs adsorbed on the TiO₂ electrode and on the glass substrate, respectively. It was found that τ_1 was the same for both kinds of substrates. However, the value of τ_2 for the CdSe QDs adsorbed on the nanostructured TiO₂ electrode was much smaller than that on the glass substrate. Under the experimental conditions (pump intensity < 2 μ J/pulse in this case), the waveforms of the responses overlapped each other very well when they were normalized at the peak intensity, as mentioned above. Therefore, it is reasonable to assume that the two decay processes in the CdSe QDs adsorbed on these two kinds of electrodes were due to one-body recombination, such as trapping, decay into intrinsic states and/or a transfer process. Because the fast decay time constant is independent of the substrates and it is known that hole trapping time is much faster than that of electron relaxation (Underwood et al., 2001; Braun et al., 2002), we believe that the fast decay process with a time scale of 2-3 ps mainly corresponded to a decrease in the photoexcited hole carrier density due to trapping at the CdSe QD surface/interface states or relaxation into the intrinsic QD states, as mentioned earlier.

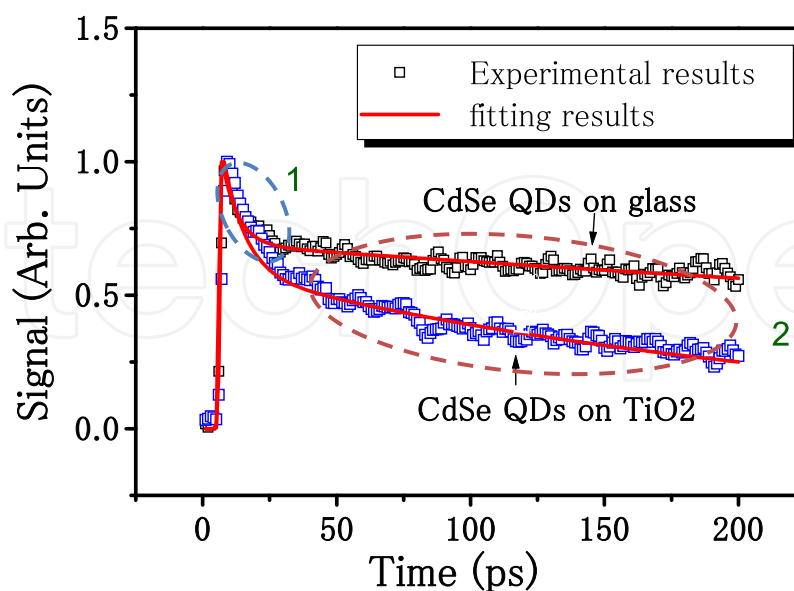


Fig. 4. TG kinetics of the CdSe QDs (average diameter: 5.5 nm) adsorbed on a nanostructured TiO₂ electrode and on a glass substrate under same adsorption conditions (Shen et al., 2008).

This result is in good agreement with the experimental results obtained with a femtosecond fluorescence up-conversion technique and transient absorption measurements (Underwood et al., 2001). The slow decay process was considered to reflect the photoexcited electron relaxation processes. For the glass substrate, no electron transfer from the QDs to the glass substrate could occur. Thus, the slow decay process only corresponded to the relaxation of photoexcited electrons in the CdSe QDs, which was mostly due to trapping at the CdSe QD surfaces. For the nanostructured TiO₂ substrate, the CdSe QDs were adsorbed onto the surfaces of the TiO₂ nanoparticles and electron transfer from the CdSe QDs to the TiO₂ nanoparticles could occur, which had been confirmed by the photocurrent measurements (Shen et al., 2004a, 2004b). As mentioned above, the TG signal due to the change in the refractive index $\Delta n(t)$ of the TiO₂ nanoparticles resulted from the injected free electrons from the CdSe QDs would be very small and can be ignored. Therefore, the slow decay process of the CdSe QDs adsorbed on the nanostructured TiO₂ film mostly reflected the decrease of the photoexcited electron densities in the CdSe QDs due to both electron trapping at the CdSe QD surfaces/interfaces and electron transfer from the CdSe QDs to the TiO₂ nanoparticles. This is the reason why the τ_2 obtained for the CdSe QDs adsorbed on the nanostructured TiO₂ electrode was much smaller than that obtained for the CdSe QDs adsorbed on the glass substrate. For the CdSe QDs on the nanostructured TiO₂ electrode, the decay rate k_2 ($k_2 = 1/\tau_2$) can be expressed as

$$k_2 = k_r + k_{et} \quad (4)$$

where k_r is the intrinsic decay rate (mostly trapping) in CdSe QDs and k_{et} is the electron-transfer rate from CdSe QDs to TiO₂. The intrinsic decay time of electrons in the CdSe QDs adsorbed on the nanostructured TiO₂ electrode was assumed to be the same as that in the CdSe QDs adsorbed on the glass substrate. In this way, we can estimate the electron transfer rate from the CdSe QDs into the nanostructured TiO₂ electrode to be approximately $5.6 \times 10^9 \text{ s}^{-1}$ using the values of τ_2 obtained from the CdSe QDs adsorbed on these two kinds of substrates. This result is very close to the electron transfer rates from CdSe QDs to TiO₂ substrates measured recently using a femtosecond transient absorption (TA) technique by Kamat and co-workers (Robel et al., 2007).

2.6 Changes of carrier dynamics in CdSe QDs adsorbed onto TiO₂ nanostructured electrodes versus adsorption conditions

The photoexcited carrier dynamics of CdSe QDs, including the electron injection rates to the TiO₂ electrodes, depends greatly on the size of the CdSe QDs, the adsorption method (mode of attachment), the adsorption conditions such as adsorption time, and the properties of the TiO₂ electrodes such as crystal structure. In the following, two examples will be introduced.

The first example is the carrier dynamics of CdSe QDs adsorbed onto TiO₂ electrodes with SILAR method (Guijarro et al., 2010a). Figure 5 shows the normalized TG kinetics of CdSe adsorbed TiO₂ electrodes with different SILAR cycles and an example of the fitting result of the TG kinetics with eq. (3) to determine the parameters A_1 , A_2 , τ_1 and τ_2 shown in Fig. 5. Figure 6 shows the dependence of τ_1 and τ_2 on the number of SILAR cycles. As shown in Fig. 6, τ_1 increases from 2.8 to 6.3 ps and τ_2 increases from 83 to 320 ps upon increasing the number of SILAR cycles from 2 to 9-15. With the SILAR cycle increasing, both the average QD size and the number of QDs increase. Therefore, for a low number of cycles, all the CdSe QDs would be in direct contact with the TiO₂ electrode, favouring electron injection.

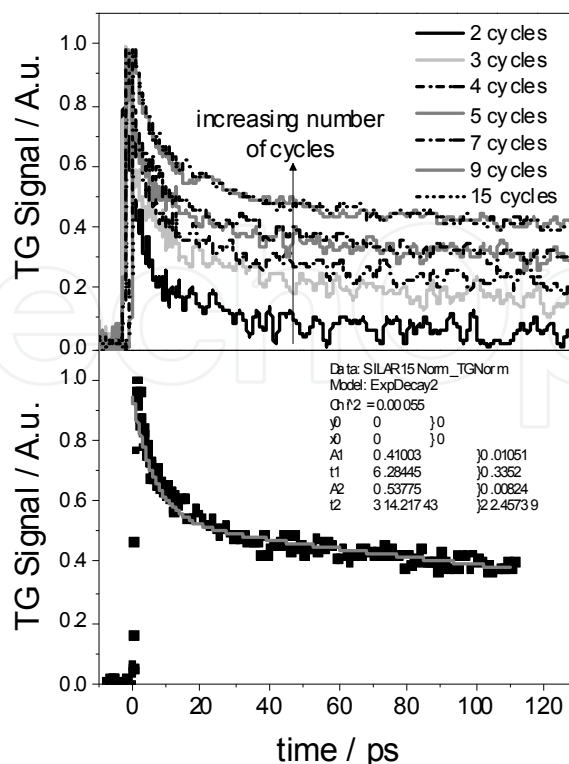


Fig. 5. Transient grating kinetics of CdSe QD adsorbed TiO₂ electrodes with different SILAR cycles (a) and an example of the fitting of the TG kinetics (15 cycles) to a double exponential decay (eq. (3)) (b) (Guijarro et al., 2010a).

However, for a large number of deposition cycles, a large fraction of CdSe QDs would not be in direct contact with the TiO₂ electrode, resulting in an increase in electron injection time. As discussed in depth by Guijarro and co-workers (Guijarro et al., 2010a), in this case, the fast decay component was attributed to direct electron transfer from the first layer of deposited CdSe QDs besides the hole trapping, and the slow one to electron injection into the TiO₂ from CdSe QDs in the outer layers (and trapping at surface and interfacial QD/QD states). For the fast decay component, the increase in QD average sizes resulted from the increase of SILAR cycles likely plays a key role in determining the values of τ_1 . The results were in qualitative agreement with those reported by Kamat and co-workers (Robel et al., 2007) showing that electron injection into TiO₂ from CdSe QDs becomes faster as the QD size gets smaller. It was considered to be due to an increase in the driving force as the CdSe conduction band shifts toward higher energies. A plot of τ_1 versus the number of SILAR cycle numbers (Fig. 6(a)) shows approximately a linear dependence. For the slow decay component, the electron relaxation time τ_2 also increases upon increasing the number of SILAR cycles (Fig. 6(b)), which can be explained as follows. The increase in the number of SILAR cycles results in not only an average increase of the CdSe quantum dot size but also an increase in the average distance of the CdSe QDs to the oxide particle. Correspondingly, the concentration of QDs not in direct contact with the TiO₂ would also grow. This leads to an increase in the average time needed for transferring the photoexcited electrons from the QDs to the oxide. Therefore, the values of A_1 and A_2 mainly reflected the relative contribution of the fast electron transfer (from the first QD layer in direct contact with the TiO₂) and the slow one (from the QDs in the outer layers), respectively. A_1 decreases from

0.84 to 0.41 while A_2 increases from 0.22 to 0.54 as the SILAR cycle increases from 2 to 9-15. For a low number of SILAR cycles, A_1 is large, indicating the predominance of electron injection from QDs in direct contact with the TiO_2 . As the SILAR cycle increases, A_2 increases because the contribution of the slower electron transfer through CdSe/CdSe interfaces becomes more and more important.

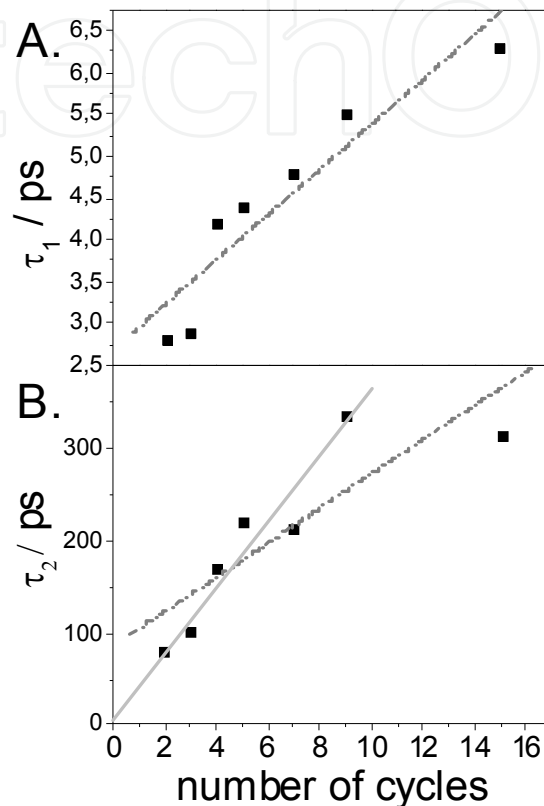


Fig. 6. Dependence of τ_1 (A) and τ_2 (B) on the number of SILAR cycles. Dashed lines correspond to linear fittings including all data, whereas the solid line shows a linear fitting forced to pass through the origin without considering the point corresponding to 15 SILAR cycles (Guijarro et al., 2010a).

The second example is the carrier dynamics of CdSe QDs adsorbed onto TiO_2 electrodes with linker-assisted (LA) method (Guijarro et al., 2010b). Figure 7 shows the TG kinetics for TiO_2 nanostructured electrodes modified by linker-adsorbed (using cysteine, p-mercaptobenzoic acid (MBA) and mercaptopropionic acid (MPA)) CdSe QDs (average size: 3.5 nm), together with the TG kinetics of the CdSe QD solution used for the adsorption. The TG kinetics of the LA adsorption samples were not sensitive to adsorption time. It indicates that the specific interaction between the thiol group (-SH) of the three kinds of linkers and the QD leads to homogeneous adsorption, in which all the QDs are adsorbed directly on the TiO_2 surface with no aggregation. As shown in Fig. 7, strong dependence of the decay of the TG kinetics on the linker nature was observed. This result suggests that, not only the length, but also other factors such as the dipole moment, the redox properties or the electronic structure of the linkers may play a role in the carrier dynamics. The TG kinetics of the LA adsorption samples were fitted very well to eq. (3),

and electron transfer rate constants were calculated according to eq. (4) by assuming that the intrinsic decay rate constant in adsorbed TiO₂ electrodes is the same as that in the CdSe colloidal dispersion (Table 2). The values of the electron transfer rate constant from CdSe to TiO₂ via MPA are in good agreement with the results obtained by Kamat's group (Robel et al., 2007), ranging from 1.0×10^9 to $2 \times 10^{11} \text{ s}^{-1}$. With respect to the effect of QD size, it was found that the smaller the QD, the faster the electron injection. Very interestingly, a direct correlation between the ultrafast carrier dynamics and the incident photon current conversion efficiency (IPCE) values measured in the absence of electron acceptors in solution for CdSe QDSCs was found. (Guijarro et al., 2010b).

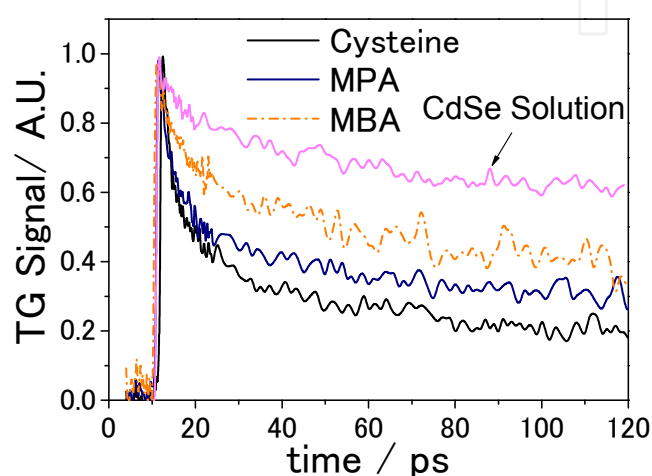


Fig. 7. TG kinetics for CdSe-sensitized TiO₂ electrodes using cysteine, MPA and MBA as linkers. All the curves are normalized to the maximum value. The TG kinetics corresponding to the CdSe solution used for LA adsorption is also given for comparison (Guijarro et al., 2010b).

| Sample | A_1 | τ_1 (ps) | A_2 | τ_2 (ps) | $k_{1,et} \times 10^{-11} \text{ (s}^{-1}\text{)}$ | $k_{2,et} \times 10^{-9} \text{ (s}^{-1}\text{)}$ |
|---------------|-----------------|---------------|-----------------|---------------|--|---|
| CdSe solution | 0.18 ± 0.01 | 8.8 ± 0.8 | 0.77 ± 0.01 | 506 ± 45 | | |
| LA (cysteine) | 0.46 ± 0.01 | 3.9 ± 0.3 | 0.41 ± 0.01 | 127 ± 7 | 1.4 ± 0.3 | 5.9 ± 0.6 |
| LA (MPA) | 0.50 ± 0.01 | 4.2 ± 0.2 | 0.46 ± 0.01 | 204 ± 13 | 1.2 ± 0.2 | 2.9 ± 0.5 |
| LA (MBA) | 0.38 ± 0.02 | 7.7 ± 0.3 | 0.77 ± 0.01 | 245 ± 24 | 0.2 ± 0.1 | 2.1 ± 0.6 |

Table 2. Fitting parameters of TG kinetics (Fig. 7) of CdSe solution and LA adsorption samples (eq. (3)) and calculated electron transfer rate constants (eq. (4)) (Guijarro et al., 2010b).

2.7 Effect of surface modification on the ultrafast carrier dynamics and photovoltaic properties of CdSe QD sensitized TiO₂ solar cells

As mentioned above, the energy conversion efficiency of QDSCs is still less than 5% at present (Mora-Sero', et al., 2010; Zhang et al., 2011) and more studies are necessary for improving the photovoltaic properties of QDSCs. The poor photovoltaic performance of QDSCs usually results from three kinds of recombination. The first one is the recombination of the injected electrons in TiO₂ electrodes with electrolyte redox species. The second one is

the recombination of photoexcited electrons in the QDs with electrolyte redox species. The third one is the recombination of photoexcited electrons and holes through surface and/or interface defects. To improve the photovoltaic performance, surface passivation should be carried out. In the previous work (Shen et al., 2008; Diguna et al., 2007a), it was found that ZnS surface coating on the CdSe QDs could improve the photovoltaic properties of CdSe QDSCs significantly. In addition to ZnS, the authors also tried surface modifications with Zn^{2+} and S^{2-} surface adsorption. The effects of the three kinds of surface modification (ZnS, Zn^{2+} , and S^{2-}) on the photovoltaic performances and ultrafast carrier dynamics of CdSe QDSCs have been investigated.

The three kinds of surface modifications for CdSe QD adsorbed TiO_2 nanostructured electrodes (24 h adsorption at 10 °C using CBD method) were carried out as follows: (1) the samples were coated with ZnS by alternately dipping them two times in 0.1 M $\text{Zn}(\text{CH}_2\text{COO})$ and 0.1 M Na_2S aqueous solutions for 1 minute for each dip; (2) the samples were adsorbed with Zn^{2+} by dipping them in 0.1 M $\text{Zn}(\text{CH}_2\text{COO})$ for 6 min; (3) the samples were adsorbed with S^{2-} by dipping them in 0.1 M Na_2S for 6 min. For characterization of the photovoltaic performances, solar cells were assembled using a CdSe QD sensitized TiO_2 electrode as the working electrode and a Cu_2S film as the counter electrode (Hodes et al., 1980). Polysulfide electrolyte (1 M S and 1 M Na_2S solution) was used as the regenerative redox couple (Shen et al., 2008b). The active area of the cells was 0.25 cm². The photovoltaic characteristics of the solar cells were measured using a solar simulator (Pecell Technologies, Inc.) at one sun (AM1.5, 100 mW/cm²). For the TG measurements, the pump and the probe wavelengths are 530 nm and 775 nm, respectively.

Figure 8 shows the photocurrent density-photovoltage curves of CdSe QDSCs, in which the QD surfaces were not modified and modified with Zn^{2+} , S^{2-} , and ZnS, respectively. The photovoltaic properties of short circuit current density, open circuit voltage and fill factor (FF) were improved after modifying the surface with ZnS or Zn^{2+} , especially the short circuit current density was improved significantly (Table 3). As a result, the energy conversion efficiencies of the samples with ZnS or Zn^{2+} surface modification increased as many as 3 times compared to the sample without surface modification. The improvement of the photovoltaic performances by means of the ZnS or Zn^{2+} surface modification may be due to (1) the decrease of surface states of TiO_2 and CdSe QDs and (2) the formation of a potential barrier at the CdSe QD/electrolyte and TiO_2 /electrolyte interfaces. However, there is little effect of the modification with S^{2-} on the photovoltaic properties. So, maybe Se^{2-} is rich on the CdSe QD surfaces.

Figure 9 shows the TG kinetics of the CdSe QD adsorbed TiO_2 electrodes before and after Zn^{2+} and ZnS surface modification. From the TG kinetics, two decay processes were observed. The fast and slow decay processes were mostly attributed to photoexcited hole trapping and electron transfer dynamics, as discussed earlier. For the sample before and after Zn^{2+} surface modification, the fast decay times were 4.5 and 2 ps, and the slow decay times were 53 ps and 25 ps, respectively. It indicates that the hole and electron relaxation became faster after the surface modification. Similar results were also obtained after the ZnS and S^{2-} surface modifications as shown in Fig. 10. The faster electron transfer due to the surface modification may result from the decrease of the surface trapping states. Further studies on the mechanism of the effects of the surface modifications on the photovoltaic performances and the carrier dynamics are in progress now.

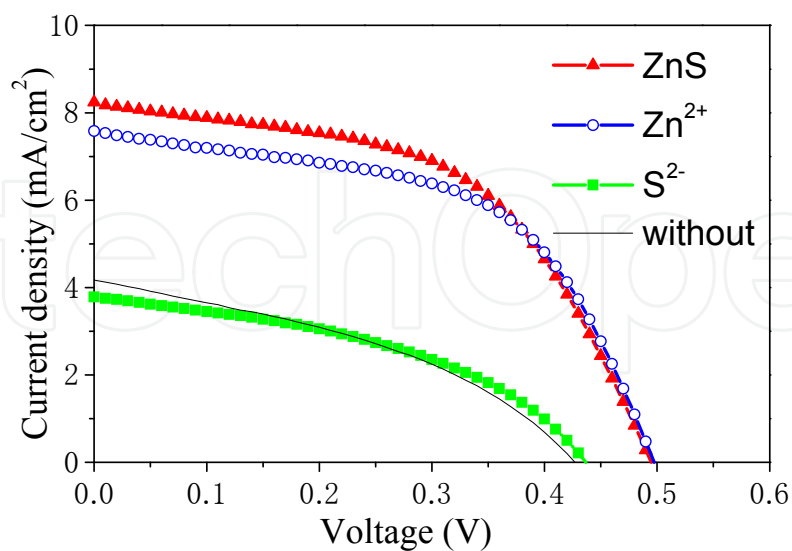


Fig. 8. Photocurrent density-photovoltage characteristics of CdSe QD-sensitized solar cells without and with surface modifications.

| Sample | J_{sc} (mA/cm ²) | V_{oc} (V) | FF | η (%) |
|---|--------------------------------|--------------|------|------------|
| TiO ₂ /CdSe | 4.2 | 0.43 | 0.39 | 0.69 |
| TiO ₂ /CdSe/ZnS | 8.2 | 0.49 | 0.53 | 2.1 |
| TiO ₂ /CdSe/Zn ²⁺ | 7.6 | 0.50 | 0.53 | 2.1 |
| TiO ₂ /CdSe/S ²⁻ | 3.8 | 0.44 | 0.43 | 0.82 |

Table 3. Photovoltaic properties of CdSe QDSCs before and after surface modifications with Zn²⁺, S²⁻, and ZnS, respectively. J_{sc} is the short circuit current density, V_{oc} is the open circuit voltage, FF is the fill factor, and η is the energy conversion efficiency.

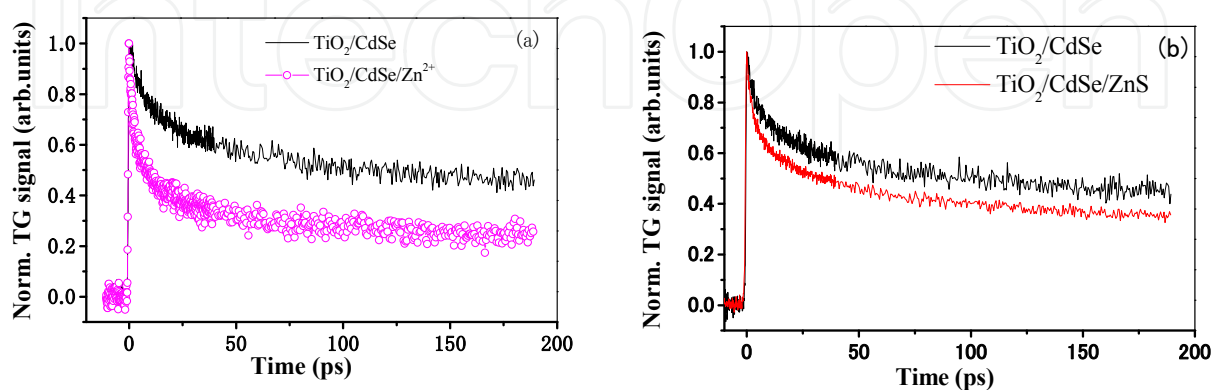


Fig. 9. Transient grating kinetics of CdSe QD adsorbed TiO₂ electrode before and after the surface modification with Zn²⁺ (a) and ZnS (b).

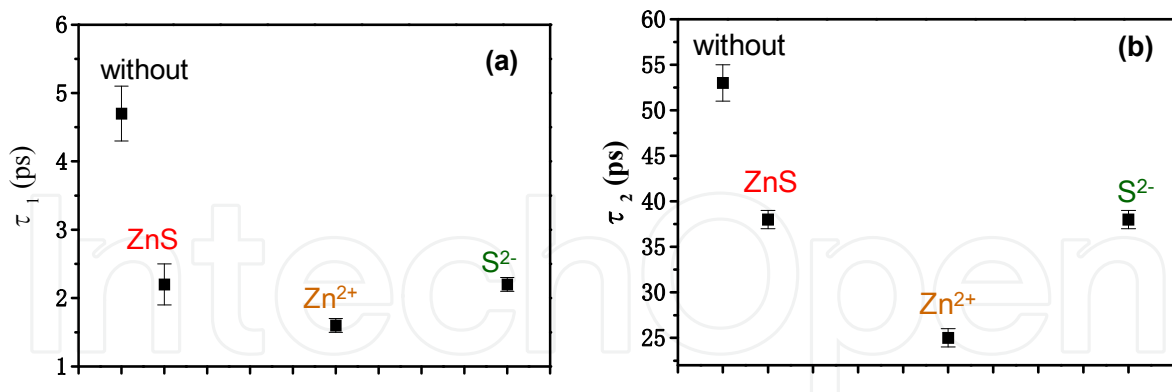


Fig. 10. Fast (τ_1) (a) and slow (τ_2) (b) decay times of the transient grating kinetics for CdSe QD adsorbed TiO₂ electrodes before and after the surface modifications with ZnS, Zn²⁺ and S²⁻.

3. Conclusion

In summary, the photoexcited carrier dynamics in CdSe QDs adsorbed onto TiO₂ nanostructured electrodes have been characterized by using the improved TG technique. It has been demonstrated that both photoexcited electron and hole dynamics can be detected by using this improved TG technique. By comparing the TG responses measured in air and in a Na₂S solution (hole acceptor), the dynamics of photoexcited electrons and holes in the CdSe QDs has been successfully separated from each other. It was found that charge separation in the CdSe QDs occurred over a very fast time scale from a few hundreds of fs in the Na₂S solution via hole transfer to S²⁻ ions to a few ps in air via hole trapping. On the other hand, the electron dynamics in the CdSe QDs, including trapping and injection to the metal oxide electrodes, depends greatly on the QD size, and adsorption methods (such as CBD, SILAR, DA and LA adsorption methods) and conditions (such as adsorption time and SILAR cycle number). In addition, surface modifications such as ZnS coating and adsorption with Zn²⁺ have been demonstrated to improve the photovoltaic properties and have a great influence on the ultrafast carrier dynamics of CdSe QDSCs. Detailed studies on the correlations between the carrier dynamics and the photovoltaic properties in QDSCs are in progress now.

4. Acknowledgment

Part of this research was supported by JST PRESTO program, Grant in Aid for Scientific Research (No. 21310073) from the Ministry of Education, Sports, Science and Technology of the Japanese Government. The authors would like to thank Dr. Kenji Katayama and Dr. Tsuguo Sawada for their help in the setup of TG equipment and also thank Mr. Yasumasa Ayuzawa for his help in some experiments. The authors are grateful to Prof. Juan Bisquert, Prof. Roberto Gómez, Mr. Néstor Guijarro, Dr. Sixto Giménez, and Dr. Iván Mora-Seró for their collaboration and help in the research.

5. References

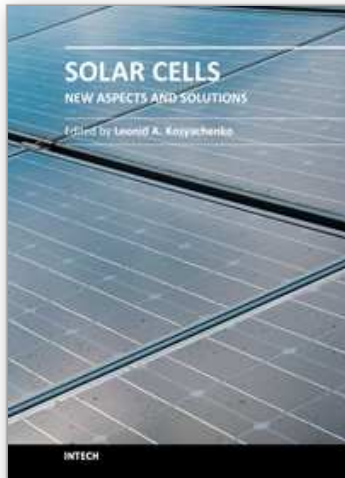
- Adachi, M.; Murata, Y.; Okada, I.; & Yoshikawa, S. (2003), *J. Electrochem. Soc.*, Vol. 150, G488.
 Bawendi, M. G.; Kortan, A. R.; Steigerwals, M.; & Brus, L. E. (1989), *J. Chem. Phys.*, Vol. 91, p. 7282.

- Blackburn, J. L.; Selmarten, D. C. & Nozik, A. J. (2003); *J. Phys. Chem. B*, Vol. 107, p. 14154.
- Blackburn, J. L.; Selmarten, D. C.; Ellingson, R. J.; Jones, M.; Micic, O. & Nozik, A. J. (2005); *J. Phys. Chem. B*, Vol. 109, p. 2625.
- Braun, M.; Link, S.; Burda C.; & El-Sayed, M. A. (2002), *Chem. Phys. Lett.*, Vol. 361, p. 446.
- Chiba, Y.; Islam, A.; Watanabe, Y.; Koyama, R.; Koide, N.; & Han, L. (2006), *Jpn. J. Appl. Phys.* Vol. 43, p. L638.
- Diguna, L. J.; Shen, Q.; Kobayashi, J.; & Toyoda, T (2007a), *Appl. Phys. Lett.*, Vol. 91, p. 023116.
- Diguna, L.J., Shen, Q., Sato, A., Katayama, K., Sawada, T., Toyoda, T. (2007b), *Mater. Sci. Eng. C*, Vol. 27, p. 1514.
- Eichler, H.J.; Gunter P. & Pohl, D. W. (1986). *Laser-induced Dynamic Gratings.*, Springer, Berlin.
- Giménez, S; Mora-Seró, I; Macor, L.; Guijarro, N.; Lala-Villarreal, T.; Gómez, R.; Diguna, L.; Shen, Q.; Toyoda, T; & Bisquert, J (2009), *Nanotechnology*, Vol. 20, p. 295204.
- Glorieux, C.; Nelson, K. A.; Hinze, G. & Fayer, M. D. (2002), *J. Chem. Phys.*, Vol. 116, p. 3384.
- Gorer, S.; & Hodes, G. (1994), *J. Phys. Chem.*, Vol. 98, p. 5338.
- Grätzel, M. (2003), *J. Photochem. Photobiol. C: Photochem. Rev.*, Vol. 4, p. 145.
- Guijarro, N.; Lana-Villarreal, T.; Mora-Seró, I.; Bisquert, J.; Gómez, R. (2009), *J. Phys. Chem. C*, Vol. 113, p. 4208.
- Guijarro, N.; Lana-Villarreal, T.; Shen, Q.; Toyoda, T. & Gómez, R. (2010a), *J. Phys. Chem. C*, Vol. 114, p. 21928.
- Guijarro, N.; Shen, Q.; Giménez, S.; Mora-Seró, I.; Bisquert, J.; Lana-Villarreal, T.; Toyoda, T. & Gómez, R. (2010b), *J. Phys. Chem. C*, Vol. 114, p. 22352.
- Hanna, M. C. & Nozik, A. J. (2006), *J. Appl. Phys.*, Vol. 100, p. 074510.
- Hodes, G; Manassen, J; & Cahen, D. (1980), *J. Electrochem. Soc.*, Vol. 127, p. 544.
- Hodes, G. (2008), *J. Phys. Chem. C*, Vol. 112, p. 17778.
- Kashiski, J. J.; Gomez-Jahn, L. A.; Faran, K. Y.; Gracewski, S. M. & Miller, R. J. D. (1989), *J. Chem. Phys.*, Vol. 90, p. 1253.
- Kamat, P. V. (2008), *J Phys Chem C*, Vol. 112, p. 18737.
- Katayama, K.; Yamaguchi, M.; & Sawada, T. (2003), *Appl. Phys. Lett.*, Vol. 82, p. 2775.
- Kim, J.; Meuer, C.; Bimberg, D. & Eisenstein, G. (2009), *Appl. Phys. Lett.*, Vol. 94, p. 041112.
- Klimov, V. I. (2006), *J. Phys. Chem. B*, Vol. 110, p. 16827.
- Law, M.; Greene, L. E.; Johnson, J. C.; Saykally, R. & Yang, P. (2005), *Nat. Mater.*, Vol. 7, p. 1133.
- Lee, Y-L.; & Lo, Y-S. (2009), *Adv. Func. Mater.*, Vol. 19, p. 604.
- L. Min, L. & Miller, R. J. D. (1990), *Appl. Phys. Lett.*, Vol. 56, p. 524.
- Miyata, R.; Kimura, Y. & Terazima, M. (2002), *Chem. Phys. Lett.*, Vol. 365, p. 406.
- Mora-Seró, I; Giménez, S; Fabregat-Santiago, F.; Gómez, R.; Shen, Q.; Toyoda, T; & Bisquert, J. (2009), *Acc. Chem. Res.*, Vol. 42, 1848.
- Mora-Seró, I & Bisquert, J. (2010), *J Phys Chem Lett*, Vol. 1, p. 3046.
- Niitsoo, O.; Sarkar, S. K.; Pejoux, P.; Rühle, S.; Cahen, D.; & Hodes, G., *J. Photochem. Photobiol. A*, Vol. 182, 306.
- Nishimura, S.; Abrams, N.; Lewis, B. A.; Halaoui, L. I.; Mallouk, T. E.; Benkstein, K. D.; Lagemaat, J. & Frank, A. K. (2003), *J. Am. Chem. Soc.*, Vol. 125, p. 6306.

- Nozik, A. J. (2002), *Physica E*, Vol. 14, p. 16827.
- Nozik, A. J. (2008), *Chem. Phys. Lett.*, Vol. 457, p. 3.
- Nozik, A. J.; Beard, M. C.; Luther, J. M.; Law, M.; Ellingson, R. J. & Johnson, J. C. (2010), *Chem. Rev.*, Vol. 110, p. 6873.
- Ohmor, T.; Kimura, Y.; Hirota, N. & Terazima, M. (2001), *Phys. Chem. Chem. Phys.*, Vol. 3, p. 3994.
- O'Regan, B.; & Grätzel (1991), *Nature*, Vol. 353, p. 737.
- Park, B.-W.; Inoue, T.; Ogomi, Y.; Miyamoto, A; Fujita, S; Pandey, S. S. & Hayase, S. (2011) *Appl. Phys. Express*, Vol. 4, p. 012301.
- Paulose, M.; Sharkar, K.; Yoriya, S.; Prakasam, H. E.; Varghese, O. K.; Mor, G. K.; Latempa, T. A.; Fitzgerald, A. & Grimes, C. A. (2006), *J. Phys Chem. B*, Vol. 110, p. 16179.
- Peter, L. M.; Riley, D. J.; Tull, E. J. & Wijayanta, K. G. U. (2002), *Chem. Commun.*, Vol. 2002, p. 1030.
- Plass, R.; Pelet, S.; Krueger, J.; Gratzel, M. & Bach, U. (2002), *J. Phys. Chem. B*, Vol. 106, p. 7578.
- Polo, A. S.; Itokatu, M. K. & Iha, N. Y. M. (2004), *Coord. Chem. Rev.*, Vol. 248, p. 1343.
- Rajesh, R. J. & Bisht, P. B. (2002), *Chem. Phys. Lett.*, Vol. 357, p. 420.
- Robel, I.; Subramanian, V.; Kuno, M. & Kamat, P. V. (2006), *J. Am. Chem. Soc.*, Vol. 128, p. 2385.
- Robel, I.; Kuno, M. & Kamat, P. V. (2007), *J. Am. Chem. Soc.*, Vol. 129, p. 4136.
- Schaller, R. D. & Klimov, V. I. (2004), *Phys. Rev. Lett.*, Vol. 92., P. 186601.
- Shen, Q.; & Toyoda, T (2003), *Thin Solid Films*, Vol. 438-439, p. 167.
- Shen, Q.; & Toyoda, T (2004a), *Jpn. J. Appl. Phys.*, Vol. 43, p. 2946.
- Shen, Q.; Arae, D.; & Toyoda, T. (2004b), *J. Photochem. Photobiol. A*, Vol. 164, p. 75
- Shen, Q.; Katayama, K.; Yamaguchi, M.; Sawada, T. & Toyoda, T. (2005), *Thin Solid Films*, Vol. 486, p. 15.
- Shen, Q.; Katayama, K.; Sawada, T.; Yamaguchi, M. & Toyoda, T. (2006a), *Jpn. J. Appl. Phys.*, Vol. 45, p. 5569.
- Shen, Q.; Sato, T.; Hashimoto, M.; Chen, C. C. & Toyoda, T. (2006b), *Thin Solid Films*, Vol. 499, p. 299.
- Shen, Q.; Yanai, M.; Katayama, K.; Sawada, T. & Toyoda, T. (2007), *Chem. Phys. Lett.*, Vol. 442, p. 89.
- Shen, Q.; Katayama, K.; Sawada, T. & Toyoda, T. (2008a), *Thin Solid Films*, Vol. 516, p. 5927.
- Shen, Q.; Kobayashi, J.; Doguna, L. J.; & Toyoda, T. (2008b), *J. Appl. Phys.*, Vol. 103, p. 084304.
- Shen, Q.; Ayuzawa, Y.; Katayama, K.; Sawada, T.; & Toyoda, T. (2010a), *Appl. Phys. Lett.*, Vol. 97, p. 263113.
- Shen, Q.; Yamada, A.; Tamura, S. & Toyoda, T. (2010b), *Appl. Phys. Lett.*, Vol. 97, p. 23107.
- Song, M. Y.; Ahn, Y. R.; Jo, S. M.; Kim, D. Y. & Ahn, J. P. (2005), *Appl. Phys. Lett.*, Vol. 87, p. 113113.
- Terazima, M.; Nogami, Y. & Tominaga, T. (2000), *Chem. Phys. Lett.*, Vol. 332, p. 503.
- Toyoda, T.; Saikusa, K. & Shen, Q. (1999), *Jpn. J. Appl. Phys.*, Vol. 38, p. 3185.
- Toyoda, T.; Sato, J. & Shen, Q. (2003), *Rev. Sci. Instrum.*, Vol. 74, p. 297.
- Vogel, R.; Pohl, K. & Weller, H. (1990), *Chem. Phys. Lett.*, Vol. 174, p. 241.

- Tvrdy, K.; Frantsuzov, P. A.; Kamat, P. V. (2011), *Proceedings of the National Academy of Sciences of the United States of America*, Vol. 108, p. 29.
- Vogel, R.; Hoyer, P. & Weller, H. (1994), *J. Phys. Chem.*, Vol. 98, p. 3183.
- Yamaguchi, M.; Katayama, K.; & Sawada, T. (2003), *Chem. Phys. Lett.*, Vol. 377, p. 589.
- Underwood, D. F.; Kippeny, T.; & Rosenthal, S. J. (2001), *Eur. Phys. J. D*, Vol. 16, p. 241.
- Yan, Y. I.; Li, Y.; Qian, X. F.; Zhu, Z. K. (2003), *Mater. Sci. Eng. B*, Vol. 103, p. 202.
- Yang, S. M.; Huang, C. H.; Zhai, J.; Wang, Z. S.; & Liang, L. (2002), *J. Mater. Chem.*, Vol. 12, p. 1459.
- Yu, P. R.; Zhu, K.; Norman, A. G.; Ferrere, S.; Frank, A. J. & Nozik, A. J. (2006), *J. Phys. Chem. B*, Vol. 110, p. 25451.
- Zhang, Q. X.; Guo, X. Z.; Huang, X. M.; Huang, S. Q.; Li, D. M.; Luo, Y. H.; Shen, Q.; Toyoda, T. & Meng, Q. B. (2011), *Phys. Chem. Chem. Phys.*, Vol. 13, p. 4659.

IntechOpen



Solar Cells - New Aspects and Solutions

Edited by Prof. Leonid A. Kosyachenko

ISBN 978-953-307-761-1

Hard cover, 512 pages

Publisher InTech

Published online 02, November, 2011

Published in print edition November, 2011

The fourth book of the four-volume edition of 'Solar cells' consists chapters that are general in nature and not related specifically to the so-called photovoltaic generations, novel scientific ideas and technical solutions, which has not properly approved. General issues of the efficiency of solar cell and through hydrogen production in photoelectrochemical solar cell are discussed. Considerable attention is paid to the quantum-size effects in solar cells both in general and on specific examples of super-lattices, quantum dots, etc. New materials, such as cuprous oxide as an active material for solar cells, AlSb for use as an absorber layer in p-i-n junction solar cells, InGaAsN as a promising material for multi-junction tandem solar cells, InP in solar cells with MIS structures are discussed. Several chapters are devoted to the analysis of both status and perspective of organic photovoltaics such as polymer/fullerene solar cells, poly(p-phenylene-vinylene) derivatives, photovoltaic textiles, photovoltaic fibers, etc.

How to reference

In order to correctly reference this scholarly work, feel free to copy and paste the following:

Qing Shen and Taro Toyoda (2011). Ultrafast Electron and Hole Dynamics in CdSe Quantum Dot Sensitized Solar Cells, *Solar Cells - New Aspects and Solutions*, Prof. Leonid A. Kosyachenko (Ed.), ISBN: 978-953-307-761-1, InTech, Available from: <http://www.intechopen.com/books/solar-cells-new-aspects-and-solutions/ultrafast-electron-and-hole-dynamics-in-cdse-quantum-dot-sensitized-solar-cells>

INTECH
open science | open minds

InTech Europe

University Campus STeP Ri
Slavka Krautzeka 83/A
51000 Rijeka, Croatia
Phone: +385 (51) 770 447
Fax: +385 (51) 686 166
www.intechopen.com

InTech China

Unit 405, Office Block, Hotel Equatorial Shanghai
No.65, Yan An Road (West), Shanghai, 200040, China
中国上海市延安西路65号上海国际贵都大饭店办公楼405单元
Phone: +86-21-62489820
Fax: +86-21-62489821

© 2011 The Author(s). Licensee IntechOpen. This is an open access article distributed under the terms of the [Creative Commons Attribution 3.0 License](#), which permits unrestricted use, distribution, and reproduction in any medium, provided the original work is properly cited.

IntechOpen

IntechOpen